PHYSICAL REVIEW B VOLUME 26, NUMBER 1 1 JULY 1982

Laplacian roughening models and two-dimensional melting

David R. Nelson
Lyman Laboratory of Physics, Harvard University, Cambridge, Massachusetts 02138
(Received 8 March 1982)

Roughening models which mimic the translational and rotational symmetries involved in two-dimensional melting are defined. One of the models is related via a duality transformation to a gas of disclinations in a solid interacting with an $r^2 \ln r$ potential. The theory of dislocation-mediated melting suggests a sequence of two continuous phase transitions for this gas and for the corresponding roughening models. Grain-boundary-mediated transitions are also possible. The roughening models are particularly amenable to computer simulations.

I. INTRODUCTION

Considerable uncertainty still surrounds the statistical mechanics of two-dimensional melting. Unlike the situation in three dimensions, analytic theories are possible,[1-4] based on a dislocation mechanism proposed by Kosterlitz and Thouless.[5,6] Dislocation pairs unbind via a continuous transition into a liquid-crystal-like hexatic phase, instead of an isotropic liquid.[2,3,7] This hexatic liquid can then transform into an ordinary liquid via an unbinding of point disclination charges.

Although some computer studies are consistent with a two-stage melting process, most simulations have been interpreted in terms of a first-order transition directly from solid to liquid.[8] Precision experiments on melting of real thin films are just beginning to be carried out. A number of experiments seem to favor dislocation-mediated melting: The melting temperature obtained by Grimes and Adams[9] for electrons on the surface of helium is in good agreement with the predictions of the dislocation theory.[10] Diffraction experiments off incommensurate methane,[11] xenon,[12] and argon[13] physiadsorbed onto graphite reveal apparently continuous melting transitions. The high-resolution x-ray radiation study of xenon, in particular, is in excellent agreement with the extension of the dislocation theory to allow for a periodic substrate.[2,3] Melting of xenon at submonolayer coverages, however, turns out to be first order.[14] Both continuous and first-order transitions appear possible.

To further clarify the melting process it would clearly be useful to have simplified statistical mechanical models, analogous to the lattice gas model of the liquid-gas critical point.[15] Such models already exist for superfluid helium films, which are believed to exhibit a *vortex* unbinding transition.[5,6,16-19] Computer simulations of "*XY*-spin-models" seem quite consistent with the Kosterlitz-Thouless picture of a vortex-mediated phase transition.[20,21] Numerical studies of interfacial roughening models,[22] which are believed to be in the same universality class as helium films,[23] have also been interpreted in this way. These simplified caricatures of reality attempt to isolate important features of the statistical mechanics. They are, moreover, not subject to the severe equilibration time difficulties which would attent the simulation of an actual helium film.

Unfortunately, the computer studies of melting mentioned earlier may also be subject to severe equilibration time problems. Equilibrium just above a dislocation unbinding transition requires times long compared to[24]

$$\tau_{\text{climb}} = \xi_T^2 / D_{\text{climb}} , \tag{1.1}$$

where ξ_T is a (diverging) translational correlation length, and D_{climb} is a diffusion constant for dislocation climb (i.e., for motion perpendicular to its Burgers vector; this requires cooperative motion of vacancies and interstitials). Because D_{climb} is quite small,[25]

$$D_{\text{climb}} \sim 10^{-10} \text{ cm}^2/\text{sec} , \tag{1.2}$$

conventional molecular dynamics simulations, with maximum run times of at most 10^{-9} sec (in argon-like units[26]), are probably incapable of following a continuous dislocation-unbinding transition. It is possible that a transition which exhibits hysteresis loops on a 10^{-9}-sec time scale, may in fact be continuous on the much longer time scales available in real experiments. (Equilibration problems may not

be so severe near a hexatic-to-liquid transition.)

In this paper we introduce a class of "Laplacian roughening" models, which mimic the translational and rotational symmetries embodied in two-dimensional melting. These systems should be no more difficult to study numerically than the usual interfacial roughening models described in Ref. 22. Problems associated with equilibration with respect to dislocation climb are avoided entirely. One of the models is dual to a gas of disclinations in a harmonic solid, which interact a $r^2 \ln r$ interaction.[27] (Two types of disclinations possible in a triangular solid are shown in Fig. 1.) In this case we argue that one might expect a transition from a phase with bound disclination quadrupoles and hexapoles to one with free *dislocations* represented by isolated disclination pairs. This phase (which corresponds to a hexatic liquid) can itself transform into a liquid phase with free disclinations. The interface in the corresponding roughening model becomes first translationally, and then orientationally disordered with increasing temperatures. Any or all of the models could also, in principle, exhibit a first-order transition.

One can also use these models to study the role of grain boundaries in melting. Fisher *et al.*[28] have discussed melting via proliferation of low- and high-angle grain boundaries. Although low-angle boundaries would probably produce a hexatic phase, large-angle boundaries would lead directly to an isotropic liquid.[28] Chui[29] has argued that grain boundaries or a coupling to density changes in a solid will *always* produce a first-order solid-liquid transition.[30]

Intriguing simulation results on a model of melting have already been presented by Saito.[31] Saito simulates a vector Coulomb gas of dislocation charges,[32] and finds a continuous transition to a hexatic liquid at high core energies, and a first-order transition at low core energies. Because this model does not include the disclination pairs buried in every dislocation core,[27] he does not see the second disclination unbinding transition expected at high core energies. Saito argues that the first-order transition at low core energies is a grain-boundary-driven melting into an isotropic liquid. Although this is certainly a plausible interpretation, it is possible that this transition is also into a hexatic phase. The hydrodynamic description of hexatics developed in Ref. 3 suggests that, if dislocations are plentiful, there will be a tendency to align in grain boundaries. Hopefully, simulations of the Laplacian roughening models (or direct numerical studies of disclinations interacting with an $r^2 \ln r$ interaction) will clarify the situation.

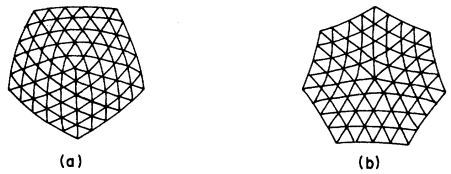

FIG. 1. Fivefold (a) and sevenfold (b) disclinations imbedded in a triangular lattice.

It is worth noting that all the models discussed above break down when the linear density of dislocations in a grain boundary approaches one per lattice constant. One then approximates a 60° grain boundary, which in a triangular solid has, in fact, zero energy. This point may provide an explanation for the grain boundaries observed, for example, by McTague *et al.*[33] in simulations of particles interacting with a repulsive $1/r^6$ potential: If the width of the hexatic phase is narrow, disclinations must unbind into an isotropic liquid when the translational correlation length is still large. Under such circumstances, they can only separate by laying down a cut in the bond angle field, i.e., a 60° grain boundary.[34] A *premature* disclination unbinding (i.e., before dislocations dissociate) of this kind was proposed as a mechanism for a first-order transition in Ref. 2.

In Sec. II A, we first define the Laplacian roughening models, and then discuss the behavior of the interfaces they describe as a function of temperature. *Two* distinct roughening transitions are possible. Section II B shows how one of the models can be mapped onto the theory of two-dimensional melting. A number of universal results for roughening correlation functions are tabulated. In Sec. II C, we discuss the behavior of Laplacian roughening models in dimensions other than $d=2$. Appendix A discusses the behavior of a Laplacian roughening model at high temperatures, and a duality relation is worked out in Appendix B. The theory of disclinations interacting in a harmonic solid is sketched in Appendix C.

II. ROUGHENING MODELS AND TWO-DIMENSIONAL SOLIDS

A. Laplacian roughening models

To motivate the models introduced here, consider first the symmetries of a two-dimensional crystal. The long-wavelength free energy of a triangular solid,[35]

$$F=\int d^2r(2\mu u_{ij}^2+\lambda u_{kk}^2)\ , \tag{2.1}$$

depends on elastic constants μ and λ, as well as on the symmetrized strain tensor

$$u_{ij}(\vec{r})=\tfrac{1}{2}[\partial_i u_j(\vec{r})+\partial_j u_i(\vec{r})]\ , \tag{2.2}$$

where $\vec{u}(\vec{r})=\vec{u}(x,y)$ is the displacement field. This free energy is invariant under a three-parameter family of continuous transformations,

$$\vec{u}(\vec{r})\rightarrow\vec{u}(\vec{r})+\vec{u}_0+\theta_0(\hat{z}\times\vec{r})\ , \tag{2.3}$$

where $\vec{u}_0$ is a uniform translation and θ_0 represents a rotation about the z axis. A $2d$ solid is characterized by quasi-long-range translational order and long-range orientational order.[36] There are two possibilities with increasing temperature: Both these symmetries can be restored at once, producing an isotropic liquid, or translational and orientational order can be eliminated sequentially, with an intervening hexatic phase. It is not possible to destroy orientational correlations without obliterating translational order, since a rotation drastically affects translational correlations between distant points.

Now consider a Hamiltonian for an integer field $h(\vec{r})$ located at the sites $\vec{r}=(x,y)$, of a triangular lattice with unit spacing, namely,

$$\mathscr{H}=-\tfrac{1}{2}J\sum_{\vec{r}}|\Delta h(\vec{r})|^p\ . \tag{2.4}$$

Here p is, for example, a positive integer, J is a positive constant, and the operator Δ creates a lattice approximation to $\nabla^2 h(\vec{r})$,

$$\Delta h(\vec{r})\equiv\tfrac{2}{3}\sum_{j=1}^{6}h(\vec{r}+\vec{\delta}_j)-4h(\vec{r})\ . \tag{2.5}$$

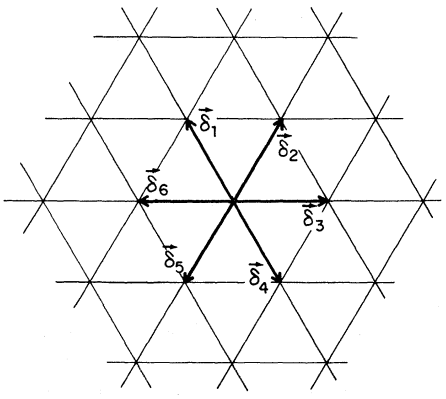

FIG. 2. Six-nearest-neighbor vectors $\vec{\delta}_j$ on a triangular lattice with unit spacing.

The $\{\vec{\delta}_j\}$ are the six triangular lattice unit vectors shown in Fig. 2. A gradient would replace the Laplacian in the usual models of interfacial roughening.[22] The partition function associated with $\mathscr{H}$ is just

$$Z\equiv\prod_{\vec{r}}\left[\sum_{h(\vec{r})=-\infty}^{\infty}\right]e^{-\beta\mathscr{H}}\ . \tag{2.6}$$

At low temperatures the discreteness of the "height" variable $h(\vec{r})$ will surely be important. One ground state consists of a flat interface oriented perpendicular to the z axis. A discrete infinity of alternative ground states can be generated by the set of transformations,

$$h(\vec{r})\rightarrow h(\vec{r})+m+\frac{1}{2\pi}\vec{G}\cdot\vec{r}\ , \tag{2.7a}$$

where m is an integer, and $\vec{G}$ is a reciprocal-lattice vector of the triangular lattice. (The partition function is in fact invariant under these transformations at all temperatures.) At sufficiently high temperatures we expect that discreteness should not matter, and that the sums in Eq. (2.6) can be replaced by integrals. The system then becomes invariant under a family of *continuous* transformations,

$$h(\vec{r})\rightarrow h(\vec{r})+h_0+\vec{c}\cdot\vec{r}\ , \tag{2.7b}$$

where h_0 represents a translation of the interface and $\vec{c}=(c_x,c_y)$ parametrizes rotations about the x and y axes. The interface now has neither a well-defined orientation nor a well-defined position. With decreasing temperatures the interface could lock into a definite orientation and position simultaneously. Alternatively, the orientation could lock first, with the interfacial position remaining "rough" or ill defined. The interface would then become smooth at a lower temperature. It is not possible to break the translational symmetry without also giving the interface a definite orientation. Evidently, there is an interesting analogy between the possible behaviors of the Laplacian roughening models with *decreasing* temperature, and the different ways of melting a two-dimensional solid with *increasing* temperature. The roles of orientational and translational degrees of freedom are reversed.

To distinguish between different phases it is convenient to introduce a correlation function which is invariant under (2.7), namely,

$$C_k(R)\equiv\langle\exp\{2\pi ik[h(\vec{r}_1)-h(\vec{r}_2)+h(\vec{r}_3)-h(\vec{r}_4)+h(\vec{r}_5)-h(\vec{r}_6)]\}\rangle\ , \tag{2.8}$$

where k is a real constant. The six points $\vec{r}_i$ form the vertices of a regular hexagon with characteristic dimension R (see Fig. 3). At low temperatures the $h(\vec{r}_i)$ assume values corresponding to a smooth, oriented interface, and we expect that $C_k(R)$ approaches a constant for large R,

$$\lim_{R\to\infty} C_k(R)=\text{const}\neq 0\ . \tag{2.9}$$

At high temperatures $h(\vec{r})$ should fluctuate wildly, since the interface has neither a definite position nor a definite orientation. For the special case $p=2$, we show in Appendix A that these fluctuations cause $C_k(R)$ to decay to zero, like the exponential of the *area* enclosed by the hexagon

$$C_k(R)\sim e^{-c(T)k^2R^2}\ , \tag{2.10a}$$

where

$$c(T)=\frac{3\pi k_BT}{2J}\ln\left[\frac{27}{16}\right]\ . \tag{2.10b}$$

A duality transformation (valid when $p=2$) to be discussed later suggests that a third, intermediate phase is possible, in which $C_k(R)$ decays *algebraically* to zero,

$$C_k(R)\sim 1/R^{k^2\eta(T)}\ , \tag{2.11}$$

with a temperature-dependent exponent $\eta(T)$. This phase corresponds to a rough, but orientationally locked interface. The correlation function $C_k(R)$ seems particularly well suited for distinguishing between the various phases in numerical simulations. Alternatively, one could study

$$-\frac{1}{4\pi^2}\frac{d^2C_k(R)}{dk^2}\bigg|_{k=0}=\left\langle\left[\sum_{j=1}^{6}(-1)^jh(\vec{r}_j)\right]^2\right\rangle. \tag{2.12}$$

Another interesting correlation function is

$$g(\vec{r})\equiv\sum_{j=1}^{6}\langle[h(\vec{r})-h(\vec{r}+\vec{\delta}_j)-h(\vec{0})+h(\vec{\delta}_j)]^2\rangle\ , \tag{2.13}$$

which measures correlations between tangents to the interface at widely separated points. In any phase with a locked interfacial orientation we expect that

$$\lim_{r\to\infty} g(r)=\text{const}<\infty\ . \tag{2.14}$$

At high temperatures one can show for $p=2$ that $g(r)$ diverges logarithmically with r (see Appendix A),

$$g(r)\underset{r\to\infty}{\approx}\frac{3}{4\pi^3}K(T)\ln(r/a)\ , \tag{2.15a}$$

where

$$K(T)=4\pi^2k_BT/J\ . \tag{2.15b}$$

The behavior of $g(r)$ for large r confirms our expectation that the interface will be orientationally rough at high temperatures.

B. Duality and phase transitions in a disclination gas

Chui and Weeks[23] have shown that the discrete Gaussian model of ordinary roughening can be mapped onto a Coulomb gas of integer changes originally solved by Kosterlitz in the context of the $2d$ XY model.[16] This mapping is a "duality transformation" in the sense that high temperatures in the roughening problem are mapped onto

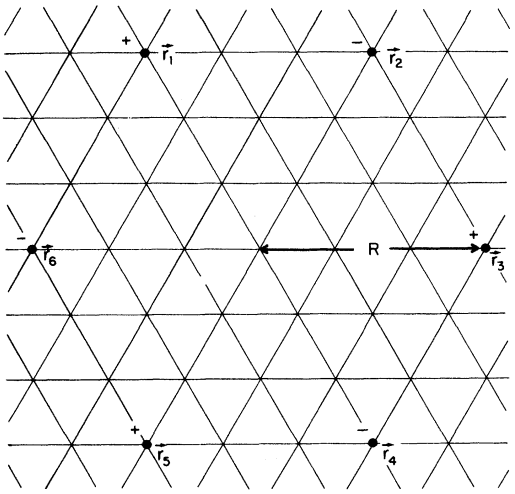

FIG. 3. Positions $\vec{r}_i$ entering the six-point height correlation function $C_k(R)$. The $\pm$ signs determine the sign of the $\{h(\vec{r}_i)\}$. The characteristic dimension of the hexagon formed by these points is R. The correlation $C_k(R)$ is related via a duality transformation to the potential of mean force between disclination charges at the vertices of this hexagon. Plus and minus signs then indicate sevenfold and fivefold disclinations, respectively.

low temperatures in the Coulomb gas, and vice versa. Analogous manipulations are applied to the partition function (2.6) in Appendix B, with the result that

$$Z \propto \left[\prod_{\vec{r}} \sum_{s(\vec{r})=-\infty}^{\infty} \right]' \exp\left[\frac{-2\pi^2 k_B T}{J} \sum_{\vec{r}\neq\vec{r}'} V(\vec{r}-\vec{r}')s(\vec{r})s(\vec{r}') \right], \tag{2.16}$$

where, for large r, the potential $V(\vec{r})$ takes the form

$$V(\vec{r}) \approx \frac{1}{8\pi}(r^2 \ln r + Ar^2 - B) . \tag{2.17}$$

The parameters A and B are positive constants, and the prime in Eq. (2.16) means that the summations are restricted to integer complexions $\{s(\vec{r})\}$ which not only are charge neutral,

$$\sum_{\vec{r}} s(\vec{r}) = 0 , \tag{2.18}$$

but also have no net dipole moment,

$$\sum_{\vec{r}} \vec{r} s(\vec{r}) = 0 . \tag{2.19}$$

Combining Eqs. (2.17) and (2.16) we obtain a large distance approximation to Z, namely,

$$Z \propto \left[\prod_{\vec{r}} \sum_{s(\vec{r})=-\infty}^{\infty} \right]' e^{-\tilde{\mathcal{H}}} , \tag{2.20a}$$

where

$$\tilde{\mathcal{H}} = \frac{K}{16\pi} \sum_{\vec{r}\neq\vec{r}'} |\vec{r}-\vec{r}'|^2 \ln|\vec{r}-\vec{r}'| s(\vec{r})s(\vec{r}') + E_c \sum_{\vec{r}} s^2(\vec{r}) \tag{2.20b}$$

and

$$K = \frac{4\pi^2 k_B T}{J}, \quad E_c = \frac{BK}{16\pi} . \tag{2.21}$$

The parameter A drops out because of the dipole neutrality condition.

Equation (2.20) looks like the partition function for a set of charges interacting via an $r^2 \ln r$ potential. The quantity E_c plays the role of a core energy. Unlike a conventional two-dimensional Coulomb gas with logarithmically interacting charges, like charges attract and unlike charges repel. As shown in Appendix C, the same partition function describes a grand canonical ensemble of disclinations interacting in a harmonic solid. This correspondence is illustrated in Fig. 4, which is taken from a computer simulation of particles interacting via a repulsive $1/r$ potential by Morf.[37] Particles whose coordination number deviates from six are indicated by asterisks and diamonds. Highlighting these special 5- and 7-coordinated particles constitutes a microscopic definition of disclinations.[38] The disclination model constructed in Appendix C keeps track of the positions and interactions of the asterisks and diamonds and allows them to be created and annihilated. The remaining particles are accounted for only to the extent that they mediate interactions between disclinations.

The behavior of this disclination gas (at least in the limit of large core energies) is a consequence of the theory of dislocated mediated melting developed in Ref. 3. As discussed in Appendix C, disclinations will be tightly bound into quartets and sextets with no net charge or dipole moment in a low-temperature solid. It is then convenient to group the disclination charges into neutral dipole pairs, which behave like *dislocations*. To see this imagine pulling a quartet apart as shown in Fig. 5, assuming that the remaining disclinations adjust to ensure overall dipole charge neutrality. It is tedious but straightforward to show that the contribution to Eq. (2.20b) of this configuration for large separations is just

$$-\frac{K}{4\pi}\left[\vec{b}_i \cdot \vec{b}_j \ln r - \frac{(\vec{b}_i \cdot \vec{r})(\vec{b}_j \cdot \vec{r})}{r^2} \right] + 2E_c(|\vec{b}_i|^2 + |\vec{b}_j|^2) , \tag{2.22}$$

where $\vec{r}$ is the separation, and

$$\vec{b}_k = \hat{z} \times \vec{\delta}_k . \tag{2.23}$$

But this is just the interaction potential between a pair of dislocations with Burger's vectors $\vec{b}_i$ and $\vec{b}_j$, core energy $2E_c$, and separation $\vec{r}$.[27] Similar results hold for arbitrary complexions of disclination pairs. The combination of the dipole neutrality constraint and the $r^2 \ln r$ potential strongly favors separated disclinations pairing into dipoles separated by a lattice constant. It is then reasonable to replace Eq. (2.20) by the partition function for a

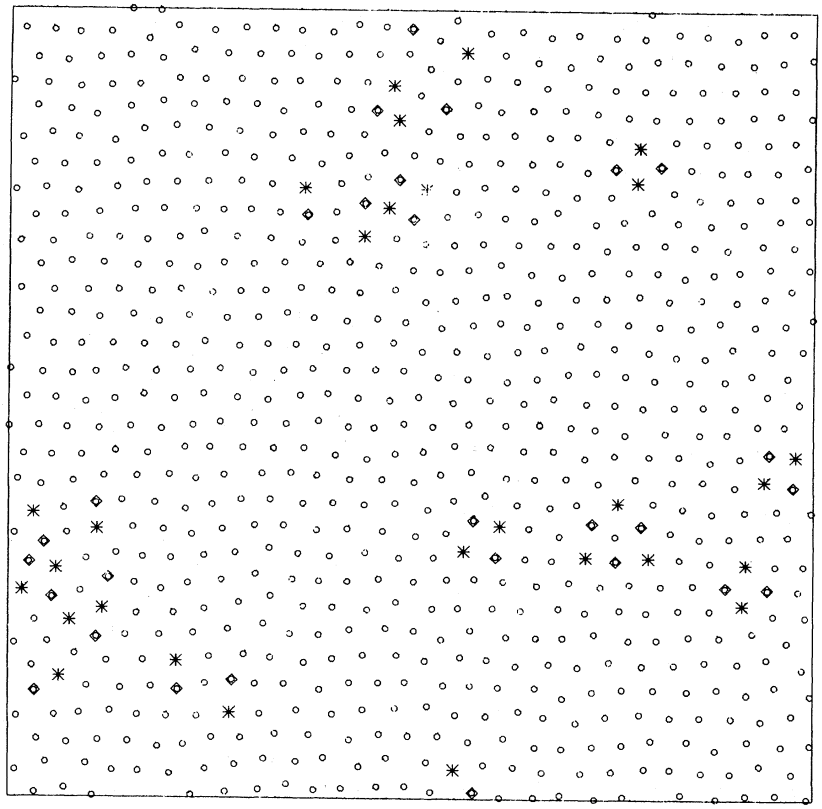

FIG. 4. Microscopic disclination "charges" in a computer simulation. Asterisks and diamonds indicate 5- and 7-coordinated particles, respectively. All other particles have coordination number 6. The picture is taken from a simulation by Morf of particles interacting with a repulsive $1/r$ potential (Ref. 37).

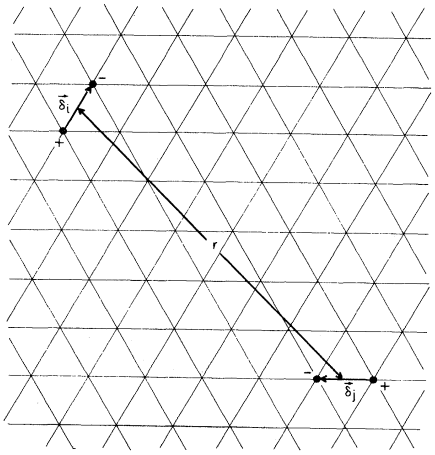

FIG. 5. A quartet of disclinations pulled apart into a pair of dipoles. For large separations the dipoles interact like two dislocations with Burgers vectors rotated by 90° with respect to the dipole moments.

logarithmically interacting dislocation gas at temperature $\tilde{T}$,

$$Z_d = \sum_{\{\vec{b}(\vec{r}_i)\}}{}' e^{-\mathcal{H}_d/k_B\tilde{T}}, \tag{2.24a}$$

where

$$\frac{\tilde{\mathcal{H}}_d}{k_B\tilde{T}} = -\frac{K}{8\pi}\sum_{i\neq j}\left[b(\vec{r}_i)\cdot b(\vec{r}_j)\ln r_{ij} - \frac{b(\vec{r}_i)\cdot\vec{r}_{ij}\,b(\vec{r}_j)\cdot\vec{r}_{ij}}{r_{ij}^2}\right]$$

$$+2E_c\sum_i |\vec{b}_i|^2 . \tag{2.24b}$$

The sum is over complexions of Burgers vectors $\vec{b}(\vec{r}_i)$ located at the *bonds* $\{\vec{r}_i\}$ of the triangular lattice, and subject to the constraint,

$$\sum_i \vec{b}(\vec{r}_i) = \vec{0} . \tag{2.25}$$

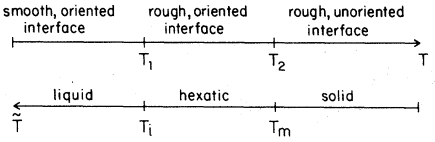

FIG. 6. Relation between the roughening temperature scale T and the temperature $\tilde{T}$ of the disclination gas provided by the duality transformation.

The "temperature" $\tilde{T}$ is inversely proportional to the temperature in the original Laplacian roughening model. Note that the Burgers vectors are automatically quantized in direction and magnitude by the underlying triangular lattice. Burgers vectors appropriate to other crystal structures could be obtained from Laplacian roughening models defined on alternative lattices.

The behavior of the vector Coulomb gas (2.24) was worked out in Refs. 2–4. Dislocation pairs unbind via an infinite-order phase transition at temperature $\tilde{T}=T_m$. Above this temperature free dislocations produce a screened, logarithmic interaction which is attractive for disclinations with opposite sign.[2,3] The effective Hamiltonian after dislocation screening is taken into account has the form[3]

$$\frac{\mathscr{H}_{\text{eff}}}{k_B\tilde{T}}=\frac{\pi K_A}{36}\sum_{\vec{r}\neq\vec{r}'}s(\vec{r})s(\vec{r}')\ln|\vec{r}-\vec{r}'|+E_c\sum_{\vec{r}}s^2(\vec{r})\,. \tag{2.26}$$

A second disclination unbinding transition occurs at a higher temperature $\tilde{T}=T_i$, leading to exponential screening at large distances. The correspondence between these two transitions and the two distinct roughening temperatures T_1 and T_2 they suggest for the Laplacian roughening models are summarized in Fig. 6.

The duality transformation for the roughening correlations $C_k(R)$ and $g(r)$ is also discussed in Appendix B. The result for $C_k(R)$ takes the form

$$C_K(R)=e^{-U_k(R)}\,, \tag{2.27}$$

where $U_k(R)$ is the renormalized interaction potential (i.e., the "potential of mean force"[39]) for six disclination test charges of strength k with alternating signs located at the vertices of the large hexagon in Fig. 3. At low temperatures $\tilde{T}$, $U_k(R)$ for large R is just

$$U_k(R)=\frac{K_R}{16\pi}k^2\sum_{j\neq j'}(-1)^{j+j'}|\vec{r}_j-\vec{r}_{j'}|^2\times\ln|\vec{r}_j-\vec{r}_{j'}|\,, \tag{2.28}$$

where K_R measures the strength of the screened disclination potential. It is easy to check that $C_k(R)$ decays as indicated in Eq. (2.10a), with

$$c(T)=\frac{3K_R}{8\pi}\ln\left[\frac{27}{16}\right]. \tag{2.29}$$

The quantity K_R was calculated in Refs. 3 and 4. At temperatures below the dislocation unbinding transition K_R is given by

$$K_R=\lim_{l\to\infty}K(l)\,, \tag{2.30}$$

where $K(l)$ is the solution of a coupled set of renormalization recursion relations,

$$\frac{dK^{-1}(l)}{dl}=\frac{3}{2}\pi y^2(l)e^{K(l)/8\pi}I_0(K(l)/8\pi))-\frac{3}{4}\pi y^2(l)e^{K(l)/8\pi}I_1(K(l)/8\pi)+O(y^3(l))\,, \tag{2.31a}$$

$$\frac{dy(l)}{dl}=\left[2-\frac{K(l)}{8\pi}\right]y(l)+2\pi y^2(l)e^{K(l)/16\pi}I_0(K(l)/8\pi)+O(y^3(l))\,. \tag{2.31b}$$

The functions $I_0(x)$ and $I_1(x)$ are Bessel functions, and the equations are to be solved subject to the initial conditions

$$K(l=0)=K,\quad y(l=0)=e^{-2E_c}\,. \tag{2.32}$$

Note from Eq. (2.24b) that $2E_c$ is the core energy for a *single* dislocation. It is a consequence of these recursion relations that K_R approaches a universal constant as $\tilde{T}\to T_m^-$,

$$\lim_{\tilde{T}\to T_m^-}K_R(\tilde{T})=16\pi\,. \tag{2.33}$$

It follows from Eq. (2.29) that $c(T)$ is universal just above the upper roughening temperature T_2,

$$\lim_{T\to T_2^+} c(T)=6\ln\left[\frac{27}{16}\right]\approx 3.139\,488\,6\ldots . \tag{2.34}$$

As shown in Appendix B, the height tangent correlation function $g(r)$ is closely related to the renormalized interaction potential between two well-separated disclination pairs. At high temperatures in the roughening model $g(r)$ should behave as in Eq. (2.15a), with K replaced by K_R. As $T\to T_2^+$ the universal prediction analogous to (2.34) is

$$g(r)\underset{r\to\infty}{\approx}\frac{12}{\pi^2}\ln r . \tag{2.35}$$

Just below T_2 the logarithmic behavior will cease for $r>\xi_T$, where ξ_T diverges as T approaches T_2 from below,[2-4]

$$\xi_T\sim e^{\text{const}/|T-T_2|^{\bar\nu}}, \tag{2.36a}$$

where

$$\bar\nu=0.369\,634\,77\ldots . \tag{2.36b}$$

The function $g(r)$ then tends to a constant given by

$$\lim_{r\to\infty} g(r)\approx\frac{12}{\pi^2}\ln(\xi_T/a)\sim\frac{1}{|T-T_2|^{\bar\nu}} . \tag{2.37}$$

This finite large-r limit signifies an oriented interface, which we expect at all temperatures below T_2.

Above the dislocation unbinding temperature, disclinations see the screened, logarithmic interaction characteristic of the hexatic phase. The corresponding potential of mean force $U_k(R)$ can be calculated using the effective Hamiltonian (2.26) and the Kosterlitz theory[16] of the two-dimensional scalar Coulomb gas. The result for large R is

$$U_k(R)=\frac{-\pi K_A^R}{36}k^2\sum_{j\neq j'}(-1)^{j+j'}\ln|\vec r_j-\vec r_{j'}| , \tag{2.38}$$

where K_A^R is a renormalized coupling calculable from Kosterlitz's recursion relations.[16,17] Summing the interactions over the hexagon formed by the $\{\vec r_j\}$, we find using Eq. (2.27) that the $C_k(R)$ decays as in Eq. (2.11), with

$$\eta=\tfrac{1}{6}\pi K_A^R . \tag{2.39}$$

The coupling K_A^R diverges like ξ_T^2 just above the dislocation unbinding temperature,[2,3] which translates into a diverging exponent η as $T\to T_2^-$ in the roughening problem,

$$\eta(T)\sim e^{\text{const}/|T-T_2|^{\bar\nu}} . \tag{2.40}$$

Just below the disclination unbinding transition at $\tilde T=T_i$, K_A approaches a universal constant[3],

$$\lim_{\tilde T\to T_i^-} K_A(\tilde T)=72/\pi . \tag{2.41}$$

The corresponding result transcribed for Laplacian roughening models is

$$\lim_{T\to T_1^+}\eta(T)=12 . \tag{2.42}$$

At temperatures below T_1, $U_k(R)$ will tend to a constant at large R. This constant diverges as $T\to T_1^-$,[40]

$$\lim_{R\to\infty} U_k(R)\approx 12k^2\ln(\xi_6/a) , \tag{2.43a}$$

where

$$\xi_6\sim e^{\text{const}/|T-T_1|^{1/2}} . \tag{2.43b}$$

If the two continuous roughening transitions at T_1 and T_2 are well separated the specific heat will exhibit two maxima, one below T_1, and one between T_1 and T_2. These maxima represent the entropy liberated by successive dislocation and disclination unbinding transitions. There are only essential singularities in thermodynamic quantities at T_1 and T_2.

Other correlations, besides $C_k(R)$ and $g(\vec r)$, might be used to characterize first-order roughening transitions. The importance of grain boundaries, for example, could be assessed by evaluating

$$\left\langle\left[\prod_s e^{2\pi ik(-1)^s h(\vec r_s)}\right]\left[\prod_s e^{-2\pi ik(-1)^s h(\vec r_s+\vec R)}\right]\right\rangle , \tag{2.44}$$

where the $\{\vec r_s\}$ are arranged in two parallel columns separated by $\vec R$ shown in Fig. 7. For $p=2$ Laplacian roughening models this goes over via the duality transformation into the renormalized interaction potential for two parallel grain boundaries, composed of dislocations with equal and opposite Burgers vectors. Each dislocation is, in turn, made up of a disclination pair. This renormalized potential would presumably exhibit interesting behavior near a grain-boundary-mediated phase transition.

C. Continuation in dimensionality

It is interesting to explore the behavior of the Laplacian roughening model with $p=2$ in the vicinity of two dimensions. The behavior of conventional roughening models near $d=2$ has been determined by Kosterlitz.[41] His analysis of the scalar Coulomb gas in d dimensions can be applied to the lower roughening transition in its entirety. There is no transition above two dimensions, and below $d=2$ one finds a finite roughening temperature T_1, with[41]

$$\xi_6 \sim 1/|T-T_1|^{\nu_6}, \tag{2.45a}$$

$$\nu_6 \approx 1/(2\sqrt{2-d}), \tag{2.45b}$$

in contrast to Eq. (2.43b).

It is straightforward to generalize the recursion relations (2.31) out of two dimensions to study the upper roughening transition. Duality now gives a gas of charges interacting with a potential which is the solution of

$$\nabla^4 V(\vec{r})=0 \tag{2.46}$$

in d dimensions. To lowest order in $\epsilon=2-d$, the recursion relations (2.31) are now

$$\frac{dK^{-1}}{dl} = -\epsilon K^{-1} + \frac{3}{2}\pi y^2 e^{K/8\pi} I_0(K/8\pi) - \frac{3}{4} y^2 e^{K/8\pi} I_1(K/8\pi), \tag{2.47a}$$

$$\frac{dy}{dl} = \left[2 - \frac{1}{2}\epsilon - \frac{K}{8\pi}\right] y + 2\pi y^2 e^{K/16\pi} I_0(K/8\pi). \tag{2.47b}$$

Although there is no fixed point describing a roughening transition above $d=2$ ($\epsilon<0$), for positive ϵ, there is a fixed point at

$$(K^*)^{-1} = \frac{1}{16\pi}[1-\pi B y^* + O(\epsilon)], \tag{2.48a}$$

$$y^* = (\epsilon/12\pi^2 A)^{1/2} + O(\epsilon), \tag{2.48b}$$

where

$$A = 2e^2 I_0(2) - e^2 I_1(2) = 21.937\ldots, \tag{2.49a}$$

$$B = e^1 I_0(2) = 6.1965\ldots. \tag{2.49b}$$

Linearizing about this point, we find both positive and negative eigenvalues

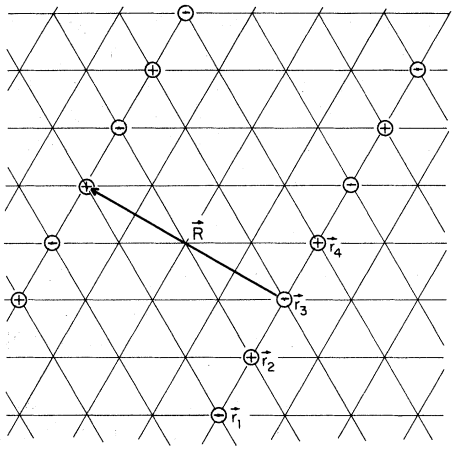

FIG. 7. Points entering the height correlation function Eq. (2.44). The plus and minus disclination charges which result from the duality transformation form a pair of parallel grain boundaries of separation $\vec{R}$.

$$\lambda_+ = \left[\frac{B}{\sqrt{12A}} + \left[\frac{B^2}{12A^{1/2}} + 4\right]^{1/2}\right]\epsilon^{1/2} = 2.418\epsilon^{1/2}, \tag{2.50a}$$

$$\lambda_- = \left[\frac{B}{\sqrt{12A}} - \left[\frac{B^2}{12A} + 4\right]^{1/2}\right]\epsilon^{1/2} = -1.654\epsilon^{1/2}. \tag{2.50b}$$

This fixed point describes a roughening transition at a temperature T_2 such that

$$\xi_T \sim \frac{1}{|T-T_2|^{\nu_T}} \tag{2.51a}$$

with

$$\nu_T = \frac{1}{2.418\epsilon^{1/2}}[1+O(\epsilon^{1/2})], \tag{2.51b}$$

which should be compared with the result (2.36) in $d=2$. The quantity ξ_T is the length scale below T_2 beyond which $V(r)$ ceases to behave like a solution of (2.46) due to screening.

It is straightforward to solve the Laplacian roughening model exactly in $d=1$ and show that the interface is both orientationally and translationally rough at all finite temperatures.[42] The absence of any roughening transitions above $d=2$ suggests that the interface is *always* orientationally and translationally locked in this case. This result can be understood in the following way: Above

$d=2$ duality no longer leads to the dipole charge neutrality condition (2.19). Consequently, free dislocation dipoles will exist at *any* finite temperature, just as in the hexatic phase. These free dipoles will screen the disclination interaction down to an effective potential

$$V_{\text{eff}}(r)\sim(r^{2-d}-1)/(2-d)\ . \tag{2.52}$$

The same kind of screening occurs in the hexatic phase in $d=2$. Above two dimensions, however, $V_{\text{eff}}(r)$ is not strong enough to bind disclinations, so that free disclinations will exist at any finite temperature. In the language of the Laplacian roughening models this means that the interface is smooth and oriented at all temperatures. Our conclusions in various dimensions are summarized in Fig. 8.

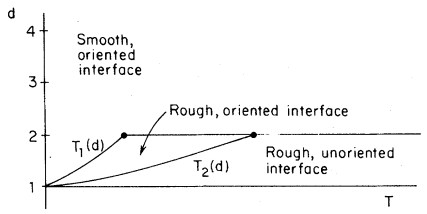

FIG. 8. Possible phases for the Laplacian roughening models as a function of temperature T and interface dimension d. For $1<d\leq 2$ there are two distinct roughening temperatures.

ACKNOWLEDGMENTS

I have benefited from conversations with D. Bruce, B. I. Halperin, and J. Tobochnik. This research was supported by the National Science Foundation through the Harvard Materials Research Laboratory and under Grant No. DMR77-10210. I would like to acknowledge a grant from the A. P. Sloan Foundation, as well as the hospitality of B. Mandelbrot and E. Pytte at the IBM Thomas J. Watson Research Center, where part of this work was carried out.

APPENDIX A: CORRELATIONS AT HIGH TEMPERATURE

To evaluate

$$C_k(R)\equiv\left\langle \exp\left[-2\pi ik\sum_{j=1}^{6}(-1)^j h(\vec{r}_j)\right]\right\rangle \tag{A1}$$

at high temperatures, we observe that it should be possible to replace sums over $h(\vec{r})$ by integrals when averaging in this limit. For $p=2$, the Hamiltonian (2.4) can be diagonalized via Fourier transformation

$$\begin{aligned}\mathscr{H}&=-\tfrac{1}{2}J\sum_{\vec{r}}[\Delta h(\vec{r})]^2\\&=-\tfrac{1}{2}J\sum_{\vec{q}}G^{-1}(\vec{q})\,|\,\hat{h}(\vec{q})\,|^2\ ,\end{aligned} \tag{A2}$$

where

$$G(\vec{q})=[4-\tfrac{4}{3}(\cos\vec{\delta}_1\cdot\vec{q}+\cos\vec{\delta}_2\cdot\vec{q}+\cos\vec{\delta}_3\cdot\vec{q})]^{-2} \tag{A3}$$

and

$$\hat{h}(\vec{q})=\frac{1}{\sqrt{\Omega}}\sum_{\vec{r}}e^{i\vec{q}\cdot\vec{r}}h(\vec{r})\ . \tag{A4}$$

The quantity Ω is the area of the system, and the wave vectors $\vec{q}$ are chosen to satisfy periodic boundary conditions. The wave vector summation in (A2) is restricted to the first Brillouin zone of the triangular lattice. It is now straightforward to show that

$$\begin{aligned}C_k(R)&=\exp\left[-2\pi^2k^2\left\langle\left[\sum_{j=1}^{6}(-1)^j h(\vec{r}_j)\right]^2\right\rangle\right]\\&=\exp\left[-2\pi^2\frac{k_BT}{J}k^2I(R)\right]\ ,\end{aligned} \tag{A5}$$

where

$$I(R)=\frac{1}{\Omega}\sum_{\vec{q}}G(\vec{q})\left|\sum_{j=1}^{6}(-1)^j e^{iR\vec{\delta}_j\cdot\vec{q}}\right|^2 \tag{A6}$$

and we have set (see Fig. 3)

$$\vec{r}_j=R\vec{\delta}_j\ . \tag{A7}$$

To extract the large-R behavior, we let

$$\vec{p}\equiv R\vec{q}\ , \tag{A8}$$

and note that

$$G(\vec{p}/R)=\frac{R^4}{p^4}[1+O(R^{-2})]\ . \tag{A9}$$

As R tends to infinity, the summation in (A6) becomes unbounded above. Taking the limit $\Omega\rightarrow\infty$, we find

$$I(R)\approx R^2\int\frac{d^2p}{4\pi^2}\frac{1}{p^4}\left|\sum_{j=1}^{6}(-1)^j e^{i\vec{\delta}_j\cdot\vec{p}}\right|^2 . \tag{A10}$$

Carrying out the angular integrations we have

$$I(R)\approx\frac{3R^2}{\pi}\int_0^\infty\frac{dp}{p^3}[1-J_0(2p)+2J_0(\sqrt{3}p) -2J_0(p)] , \tag{A11}$$

where $J_0(x)$ is a Bessel function. The remaining integral can be evaluated exactly imposing a lower cutoff, rescaling the arguments of the Bessel functions, and then sending this cutoff to zero. The result is

$$I(R)\underset{R\to\infty}{\approx}\frac{3}{4\pi}\ln\left[\frac{27}{16}\right]R^2 , \tag{A12}$$

which, when combined with (A5), is just Eq. (2.10).

Similar manipulations applied to

$$g(\vec{r})=\sum_{j=1}^{6}\langle[h(\vec{r})-h(\vec{r}+\vec{\delta}_j)-h(\vec{0})+h(\vec{\delta}_j)]^2\rangle \tag{A13}$$

suffice to show that

$$g(\vec{r})=\frac{4k_BT}{J}\frac{1}{\Omega} \times\sum_{\vec{q}}G(\vec{q})\sum_{j=1}^{6}(1-e^{i\vec{q}\cdot\vec{\delta}_j})(1-e^{i\vec{q}\cdot\vec{r}}) , \tag{A14}$$

which for large r and in the limit $\Omega\to\infty$ may be written

$$g(\vec{r})\approx\frac{6k_BT}{J}\int_{BZ}\frac{d^2q}{4\pi^2}\frac{1}{q^2}(1-e^{i\vec{q}\cdot\vec{r}}) , \tag{A15}$$

where the integral is restricted to the Brillouin zone. It is now straightforward to demonstrate that, as r tends to ∞,

$$g(\vec{r})\approx\frac{3k_BT}{\pi J}\ln r . \tag{A16}$$

APPENDIX B: DUALITY TRANSFORMATION

The duality transformation of the Laplacian roughening model for $p=2$ makes use of the Poisson summation formula,[43] which asserts that

$$\sum_{h=-\infty}^{\infty}f(h)=\sum_{s=-\infty}^{\infty}\int_{-\infty}^{\infty}dh\,f(h)e^{2\pi ish} , \tag{B1}$$

for any function $f(h)$. Applying this formula to each of the sums in Eq. (2.6) we obtain

$$Z=\prod_{\vec{r}}\left[\sum_{s(\vec{r})=-\infty}^{\infty}\int_{-\infty}^{\infty}dh(\vec{r})\right] \times\exp\left[-\beta\mathscr{H}+2\pi i\sum_{\vec{r}}s(\vec{r})h(\vec{r})\right] . \tag{B2}$$

Just as in Ref. 23, the h field is easily integrated out by first passing to the Fourier representation defined in Appendix A. The resulting expression for Z may be written

$$Z=Z_0\left[\prod_{\vec{r}}\sum_{s(r)=-\infty}^{\infty}\right] \times\exp\left[\frac{-2\pi^2k_BT}{J}\sum_{\vec{q}}G(\vec{q})\hat{s}(\vec{q})\hat{s}(-\vec{q})\right] , \tag{B3}$$

where

$$Z_0=\prod_{\vec{q}}\left[\frac{2\pi k_BT}{J}G(\vec{q})\right]^{1/2} , \tag{B4}$$

$$\hat{s}(\vec{q})=\frac{1}{\sqrt{\Omega}}\sum_{\vec{r}}e^{i\vec{q}\cdot\vec{r}}s(\vec{r}) , \tag{B5}$$

and $G(\vec{q})$ is given by Eq. (A3). Because $G(\vec{q})$ diverges like q^{-4} at small momenta there are constraints on the allowed values of the $\{s(r)\}$. To see this we rewrite the summation in (B3),

$$\sum_{\vec{q}}G(\vec{q})\hat{s}(\vec{q})\hat{s}(-\vec{q}) =\sum_{r\neq r'}V(\vec{r}-\vec{r}')s(\vec{r})s(\vec{r}')+\frac{1}{\Omega}\sum_{\vec{q}}G(\vec{q})\left[\sum_{\vec{r}}s(\vec{r})\right]^2+\frac{1}{\Omega}\sum_{\vec{q}}q_iq_jG(\vec{q})\left[\sum_{\vec{r}}r_is(\vec{r})\right]\left[\sum_{\vec{r}'}r'_js(\vec{r}')\right] -\frac{1}{\Omega}\sum_{\vec{q}}q^2G(\vec{q})\left[\sum_{\vec{r}}r^2s(\vec{r})\right]\left[\sum_{\vec{r}}s(\vec{r})\right] , \tag{B6}$$

where

$$V(\vec{r})=\frac{1}{\Omega}\sum_{\vec{q}} G(\vec{q})[e^{i\vec{q}\cdot\vec{r}}+\tfrac{1}{2}(\vec{q}\cdot\vec{r})^2-1]\ . \tag{B7}$$

The potential $V(\vec{r})$ is finite for all $r<\infty$, but the sums in the second and third terms of (B6) diverge in the thermodynamic limit unless

$$\sum_{\vec{r}} s(\vec{r})=0 \tag{B8}$$

and

$$\sum_{\vec{r}} \vec{r}s(\vec{r})=0\ . \tag{B9}$$

When these constraints are imposed in the limit $\Omega\to\infty$ the last term also vanishes and we have

$$Z=Z_0\left[\prod_{\vec{r}}\sum_{s(\vec{r})=-\infty}^{\infty}\right]'\exp\left[\frac{-2\pi^2 k_B T}{J}\sum_{\vec{r}\neq\vec{r}'} V(\vec{r}-\vec{r}')s(\vec{r})s(\vec{r}')\right]\ . \tag{B10}$$

The prime indicates that the constraints (B8) and (B9) must be respected. It is straightforward to show that, for large r,

$$V(\vec{r})\approx\frac{1}{8\pi}(r^2\ln r+Ar^2-B)\ , \tag{B11}$$

where A and B are positive constants sensitive to the details of the triangular lattice Brillouin zone. Note from (B7) that $V(r)$ vanishes for $r=0$.

The duality transformation also applies to the correlations functions defined in the text. Equation (2.8) becomes

$$C_k(R)=\exp\left[\frac{-2\pi^2 k_B T}{J}\sum_{j\neq j'} k^2(-1)^{j+j'}V(\vec{r}_j-\vec{r}_{j'})\right]\left\langle\exp\left[\frac{4\pi^2 k_B T}{J}\sum_{j=1}^{6}\sum_{\vec{r}} k(-1)^j s(\vec{r})V(\vec{r}-\vec{r}_j)\right]\right\rangle'\ , \tag{B12}$$

where the prime indicates that the average is to be taken over an ensemble specified by a probability distribution

$$\mathcal{P}(\{s(r)\})\propto\exp\left[\frac{-2\pi^2 k_B T}{J}\sum_{\vec{r}\neq\vec{r}'} V(\vec{r}-\vec{r}')s(\vec{r})s(\vec{r}')\right]\ , \tag{B13}$$

subject, however, to the constraints (B8) and (B9). Equation (B12) is the "potential of mean force"[40] associated with six disclination test charges k with alternating sign introduced at the vertices of the hexagon in Fig. 3. From (B11), it follows that the prefactor in (B12) is just the high-temperature result for $C_k(R)$ derived in Appendix A. Corrections due to finite temperatures are provided by the second factor.

To transform the correlation (2.13) it is convenient to define

$$\mathcal{G}_k(\vec{r})\equiv\sum_{j=1}^{6}\langle\exp\{2\pi ik[h(\vec{r})-h(\vec{r}+\vec{\delta}_j)-h(\vec{O})+h(\vec{\delta}_j)]\}\rangle \tag{B14}$$

and note that the desired correlation function is

$$g(\vec{r})=-\frac{1}{4\pi^2}\frac{d^2}{dk^2}\mathcal{G}_k(\vec{r})\bigg|_{k=0}\ . \tag{B15}$$

In analogy with the result (B12), we find

$$\mathcal{G}_k(\vec{r})=\sum_{j=1}^{6}\exp\left[\frac{-4\pi^2 k_B T}{J}k^2[V(\vec{r}+\vec{\delta}_j)+V(\vec{r}-\vec{\delta}_j)-2V(\vec{r})-2V(\vec{\delta}_j)]\right]$$
$$\times\left\langle\exp\left[\frac{-4\pi^2 k_B T}{J}\sum_{\vec{r}'}ks(\vec{r}')[V(\vec{r}'-\vec{r})-V(\vec{r}'-\vec{r}-\vec{\delta}_j)-V(\vec{r}')+V(\vec{r}'-\vec{\delta}_j)]\right]\right\rangle' . \quad \text{(B16)}$$

Using (B15) it can be shown that the first term of (B16) leads to the high-temperature result for $g(r)$ quoted in Appendix A.

APPENDIX C: DISCLINATIONS IN A HARMONIC SOLID

Singular solutions which minimize the continuum elastic free energy (2.1) for an isotropic solid have been discussed by Nabarro.[26] In general, the displacements $u(x,y)$ for a singularity located at the origin may be written

$$u_x(\vec{r})=-\frac{1}{2\mu}\frac{\partial\chi(\vec{r})}{\partial x}+\frac{2\mu+\lambda}{\mu(\mu+\lambda)}P(\vec{r}) , \quad \text{(C1)}$$

$$u_y(\vec{r})=-\frac{1}{2\mu}\frac{\partial\chi(\vec{r})}{\partial y}+\frac{2\mu+\lambda}{\mu(\mu+\lambda)}Q(\vec{r}) , \quad \text{(C2)}$$

where

$$\chi=xP+yQ+R . \quad \text{(C3)}$$

The functions P, Q, and R are harmonic, and P and Q are harmonic conjugates. The solution corresponding to a disclination (called a "dislocation of Volterra's sixth order" by Nabarro) has[26]

$$P(\vec{r})=Dx\ln(r/a)-Dy\tan^{-1}y/x , \quad \text{(C4)}$$

$$Q(\vec{r})=Dy\ln(r/a)+Dx\tan^{-1}y/x , \quad \text{(C5)}$$

$$\chi(\vec{r})=Dr^2\ln(r/a) , \quad \text{(C6)}$$

where D is a constant determined below, and a is a microscopic cutoff. To see that the corresponding displacements are indeed just those of a disclination, we compute the local rotation

$$\theta(\vec{r})\equiv\tfrac{1}{2}(\partial_x u_x-\partial_y u_x)$$
$$=\frac{2\mu+\lambda}{2\mu(\mu+\lambda)}\left[\frac{\partial P}{\partial y}-\frac{\partial Q}{\partial x}\right]$$
$$=-\frac{2\mu+\lambda}{\mu(\mu+\lambda)}D\tan^{-1}y/x . \quad \text{(C7)}$$

Disclinations in a triangular solid are characterized by a nonzero line integral of the "twist" $\theta(\vec{r})$ (see Fig. 1),

$$\oint d\theta(\vec{r})=\frac{2\pi}{6}s, \quad s=\pm1,\pm2,\ldots \quad \text{(C8)}$$

where the contour is any counterclockwise path enclosing the origin. This constraint will be satisfied, provided we choose

$$D=\frac{-\frac{1}{6}\mu(\mu+\lambda)}{2\mu+\lambda}s , \quad \text{(C9)}$$

where s characterizes the strength of the disclination at the origin.

For harmonic solids we can obtain χ, P, and Q for an array of disclinations with integer charges s_j at positions $\{r_j\}$ by a superposition. The function $\chi(\vec{r})$, for example, is

$$\chi(\vec{r})=\frac{-\frac{1}{6}\mu(\mu+\lambda)}{2\mu+\lambda}\sum_j s_j|\vec{r}-\vec{r}_j|^2\times\ln(|\vec{r}-\vec{r}_j|/a) , \quad \text{(C10)}$$

which satisfies the useful relation

$$\nabla^4\chi=\frac{-\frac{4}{3}\pi\mu(\mu+\lambda)}{2\mu+\lambda}\sum_j s_j\delta(\vec{r}-\vec{r}_j) . \quad \text{(C11)}$$

The strain field $u_{ij}(\vec{r})$ can be decomposed into smooth and singular parts,

$$u_{ij}(\vec{r})=\phi_{ij}(\vec{r})+u_{ij}^{\text{sing}}(\vec{r}) , \quad \text{(C12)}$$

where[26]

$$u_{ij}^{\text{sing}}=\frac{1}{2\mu}\sigma_{ij}^{\text{sing}}-\frac{\lambda}{4\mu(\mu+\lambda)}\sigma_{kk}^{\text{sing}}\delta_{ij} \quad \text{(C13)}$$

and

$$\sigma_{ij}^{\text{sing}}(r)=\epsilon_{ik}\epsilon_{jl}\partial_k\partial_l\chi(\vec{r}) . \quad \text{(C14)}$$

Inserting this decomposition into the continuum elastic free energy (2.1), we find that

$$F=\tfrac{1}{2}\int d^2r(2\mu\phi_{ij}^2+\lambda\phi_{kk}^2)+F_{\text{sing}} , \quad \text{(C15)}$$

with

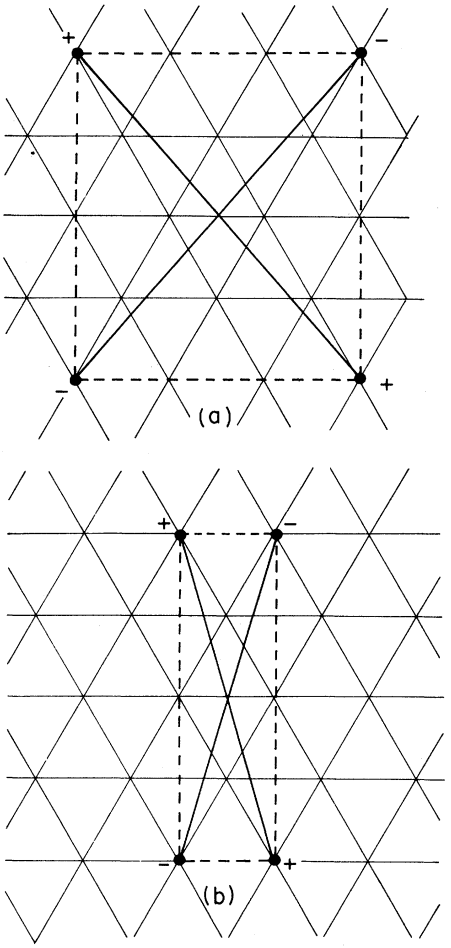

FIG. 9. Interactions between disclination charges at the vertices of a rectangle. Because the force between disclinations *increases* with distance, the interactions along the diagonals of the rectangle dominate.

$$F_{\text{sing}}=\frac{1}{\mu}\int d^2r\left[\left[\frac{\partial^2\chi}{\partial r_i\partial r_j}\right]^2-\frac{\lambda}{2(\mu+\lambda)}(\nabla^2\chi)^2\right]. \tag{C16}$$

It is straightforward to show that the energy of a configuration of disclination charges is only finite provided that

$$\sum_j s_j=0\,, \tag{C17a}$$

$$\sum_j \vec{r}_j s_j=0\,. \tag{C17b}$$

Upon imposing these constraints one can integrate by parts in (C16) and find that

$$F_{\text{sing}}=\frac{2\mu+\lambda}{4\mu(\mu+\lambda)}\int d^2r\chi\nabla^4\chi\,. \tag{C18}$$

Inserting Eqs. (C10) and (C11) into this result, we find that the free energy contributed by the interacting disclinations is

$$F_{\text{sing}}=\frac{\pi}{18}\frac{\mu(\mu+\lambda)}{2\mu+\lambda}\sum_{i\neq j}s_i s_j\,|\,\vec{r}_i\vec{r}_j\,|^2 \times\ln(\,|\,\vec{r}_i-\vec{r}_j\,|\,/a)\,. \tag{C19}$$

The partition function (2.20) in the text is just a lattice approximation to the grand canonical partition function associated with (C19). The parameter E appearing in Eq. (2.20b) acts like a core energy or chemical potential for the disclinations.

It is worth commenting on the sign of the disclination interaction which appears in Eq. (C19). Evidently, disclinations of *like* sign attract and those of *unlike* sign repel, contrary to one's intuitive expectation from, for example, Fig. 4. The explanation of this perplexing result lies in the dipole charge neutrality condition and the strength of the $r^2\ln r$ potential. An isolated disclination pair cannot be separated without violating Eq. (C17b). We are led to consider configurations like the quartet of charges shown in Fig. 9(a), which admits distortions preserving this constraint. The four interactions along the edges of the rectangle are repulsive. Because the force associated with an $r^2\ln r$ potential actually *increases* with distance, however, the attractive interactions along the diagonals dominate. The net force increases linearly with the dimension of the rectangle and will tend to produce a tightly bound quartet. If a tightly bound quartet separates at all, it is energetically preferable to do so by creating two separated dipoles, as shown in Fig. 9(b). As discussed in Sec. II, these dipoles behave like logarithmically interacting dislocations with equal and opposite Burgers vectors. In order for the net force between these dipoles to be attractive the sign of the $r^2\ln r$ potential in (C19) must be positive.

[1]D. R. Nelson, Phys. Rev. B 18, 2318 (1978).
[2]B. I. Halperin and D. R. Nelson, Phys. Rev. Lett. 41, 121; 41, 519(E) (1978).
[3]D. R. Nelson and B. I. Halperin, Phys. Rev. B 19, 2457 (1979).
[4]A. P. Young, Phys. Rev. B 19, 1855 (1979).
[5]J. M. Kosterlitz and D. J. Thouless, J. Phys. C 6, 1181 (1973).
[6]J. M. Kosterlitz and D. J. Thouless, in *Progress in Low Temperature Physics,* edited by D. F. Brewer (North-Holland, Amsterdam, 1978), Vol. VII B.
[7]A similar result would hold in three dimensions, if the dislocation loop melting mechanism proposed by Shockly [W. Shockley, *L'Etat Solid,* Proceedings of the Neuvième Conseil de Physique, Brussels, edited by R. Stoops (Institute International de Physique Solvay, Brussels, 1952)] were correct. See D. R. Nelson and J. Toner, Phys. Rev. B 24, 363 (1981).
[8]See, e.g., work reported in *Ordering in Two Dimensions,* edited by S. Sinha (North-Holland, New York, 1980).
[9]C. C. Grimes and G. Adams, Phys. Rev. Lett. 42, 795 (1979).
[10]R. Morf, Phys. Rev. Lett. 43, 931 (1979).
[11]P. Dutta, S. K. Sinha, P. Vora, M. Nielsen, L. Passell, and M. Bretz, Ref. 8, p. 169.
[12]P. A. Heiney, R. J. Birgeneau, G. S. Brown, P. M. Horn, D. E. Moncton, and P. W. Stephens, Phys. Rev. Lett. 48, 104 (1982).
[13]J. P. McTauge, J. Als-Nielsen, J. Bohr, and M. Nielsen (unpublished).
[14]A. Thomy and X. Duval, J. Chem. Phys. 67, 1101 (1970).
[15]See, e.g., H. E. Stanley, *Introduction to Phase Transitions and Critical Phenomena* (Oxford University Press, New York, 1971).
[16]J. M. Kosterlitz, J. Phys. C 7, 1046 (1974).
[17]D. R. Nelson and J. M. Kosterlitz, Phys. Rev. Lett. 39, 1201 (1977).
[18]D. J. Bishop and J. D. Reppy, Phys. Rev. Lett. 40, 1727 (1978).
[19]I. Rudnick, Phys. Rev. Lett. 40, 1454 (1978).
[20]J. Tobochnik and G. V. Chester, Phys. Rev. B 20, 3761 (1979).
[21]M. Suzuki, in *Physics of Low-Dimensional Systems,* Proceedings of the Kyoto Summer Institute, Kyoto, 1978, edited by Y. Nagaoka and S. Hikami (Publication Office, Progress in Theoretical Physics, Kyoto, 1979), p. 37.
[22]J. D. Weeks, in *Ordering in Strongly Fluctuating Condensed Matter Systems,* edited by T. Riste (Plenum, New York, 1980), p. 293, and references therein.
[23]S. T. Chui and J. D. Weeks, Phys. Rev. B 14, 4978 (1976).
[24]A. Zippelius, B. I. Halperin, and D. R. Nelson, Phys. Rev. B 22, 2514 (1980).
[25]See, e.g., R. Bruinsma, B. I. Halperin, and A. Zippelius, Phys. Rev. B 25, 579 (1982).
[26]J. P. Hansen and I. R. McDonald, *Theory of Simple Liquids* (Academic, London, 1976).
[27]F. R. N. Nabarro, *Theory of Dislocations* (Clarendon, New York, 1967).
[28]D. S. Fisher, B. I. Halperin, and R. Morf, Phys. Rev. B 20, 4692 (1979). A similar mechanism for melting was proposed in three dimensions by N. F. Mott and R. W. Gurney, Trans. Faraday Soc. 35, 364 (1939).
[29]S.-T. Chui, Phys. Rev. Lett. 48, 933 (1982).
[30]The nature of a *strongly* first-order transition will surely depend on microscopic details like the range of the interparticle potentials, etc. For *weakly* first-order transitions, however, it may make sense to search for more universal, "generic" mechanisms like grain boundaries.
[31]Y. Saito, Phys. Rev. Lett. 48, 1114 (1982).
[32]The ingredients of a corresponding roughening model can be found in Appendix A of Ref. 1.
[33]J. P. McTague, D. Frenkel, and M. P. Allen, in *Ordering in Two Dimensions,* edited by S. Sinha (North-Holland, New York, 1980).
[34]M. Kleinman, in *Dislocations in Solids,* edited by F. R. N. Nabarro (North-Holland, New York, 1980), p. 243.
[35]L. D. Landau and E. M. Lifshitz, *Theory of Elasticity* (Pergamon, New York, 1970).
[36]See, e.g., Ref. 3, and references therein.
[37]R. Morf, in *Physics of Intercalation Compounds,* edited by L. Pietronero and E. Tosatti (Springer, New York, 1981).
[38]See Ref. 33 and F. Spaepen, J. Non-Cryst. Solids 31, 207 (1978).
[39]See, e.g., D. A. McQuarrie, *Statistical Mechanics* (Harper and Row, New York, 1976).
[40]T. Ohta and K. Kawasaki, Prog. Theor. Phys. 60, 365 (1978).
[41]J. M. Kosterlitz, J. Phys. C 10, 3753 (1977).
[42]D. Bruce and D. R. Nelson (unpublished).
[43]I. M. Gel'fand and G. E. Shilov, *Generalized Functions* (Academic, New York, 1964), Vol. I, p. 332.